Cancer Cell International

RESEARCH

Open Access

Prognostic value and immune infiltration of a tumor microenvironment-related PTPN6 in metastatic melanoma

Rongyao Sun[1], Shuqiang Wei[2], Ying Yu[1], Zhuo Wang[1], Tonghao Yao[1], Yining Zhang[1], Luping Cui[1] and Xu Ma[1*]

Abstract

Background Cutaneous melanoma is one of the most invasive and lethal skin malignant tumors. Compared to primary melanoma, metastatic melanoma (MM) presents poorer treatment outcomes and a higher mortality rate. The tumor microenvironment (TME) plays a critical role in MM progression and immunotherapy resistance. This study focuses on the role of the TME-related gene PTPN6 in the prognosis and immunotherapy response of MM.

Methods This study analyzed the RNA-seq and clinical data of MM patients from public databases, employing the ESTIMATE algorithm and bioinformatics tools to identify differentially expressed genes in the TME. PTPN6 was identified as a prognostic biomarker. Its expression and function were validated using in vitro and in vivo experiments. The role of PTPN6 in immune cell infiltration and its association with the JAK2-STAT3 pathway and immunotherapy response were also evaluated.

Results PTPN6 expression was significantly lower in MM and associated with poor prognosis. In vitro, Overexpression of PTPN6 inhibited proliferation, migration, and invasion, while knockdown reversed these effects. In vivo, PTPN6 overexpression reduced tumor growth. Mechanistically, PTPN6 suppressed JAK2-STAT3 signaling pathway activation. High PTPN6 expression was positively associated with immune cell infiltration, improved immunotherapy response, and reduced PD-L1 expression.

Conclusion The gene PTPN6, associated with the tumor microenvironment, may serve as a promising prognostic biomarker and therapeutic target for MM.

Keywords Metastatic melanoma, Tumor microenvironment, PTPN6, JAK2-STAT3, Immunotherapy

*Correspondence:
Xu Ma
doctormaxu@163.com
[1]Department of Plastic and Aesthetic Surgery, the Second Affiliated Hospital of Harbin Medical University, Harbin 150086, China
[2]Department of Burn and Plastic Surgery, Qingdao Central Hospital, University of Health and Rehabilitation Sciences, Qingdao 266042, China

Introduction

Despite its low incidence, melanoma is one of the most aggressive skin cancers, accounting for nearly 90% of all skin malignant tumor deaths [1]. Early primary melanoma patients can achieve a good prognosis after surgical resection [2]. However, advanced metastatic melanoma presents a significant challenge as it is highly invasive and spreads rapidly to vital organs like the liver, lungs, and brain [3]. Therefore, these tumors are difficult to completely remove through surgery, and the recurrence rate after surgery is high. Furthermore, these tumors show insensitivity to radiotherapy and chemotherapy and quickly develop resistance to targeted therapies [4]. The 5-year survival rate is only 25% [5]. However, recent advances in immunotherapy have offered new hope in treating melanoma. Metastatic melanoma (MM) has strong immunogenicity, generating numerous tumor antigens that activate the body's immune response, making it particularly receptive to immunotherapy [3]. The advent of immune checkpoint inhibitors (ICIs), like anti-cytotoxic T-lymphocyte-associated protein 4 (CTLA-4) antibodies and anti-programmed death 1/programmed death-ligand 1 (PD-1/PD-L1) antibodies, has been effective in prolonging the survival time of melanoma patients and improving their quality of life. These treatments have significantly improved prognosis and are now the standard care for advanced metastatic melanoma.

However, a significant proportion of patients either fail to respond or develop resistance to immunotherapy, a situation heavily influenced by the complex tumor microenvironment (TME) of MM [6, 7]. Recently, there has been a growing interest in TME due to its complex composition and dynamic nature, which are pivotal in cancer development and progression [8–10]. The TME is the major site at which tumor cells interact with the host immune system, encompassing not only the tumor cells but also the stromal cells, immune cells, and the bioactive substances and extracellular matrix they produce [9, 10]. Therefore, gaining a comprehensive understanding of MM's tumor microenvironment, unraveling the biological mechanisms of the interactions within the TME, and identifying prognostic biomarkers based on the TME is crucial. Such insights could significantly aid in inhibiting MM's development, enhancing patient prognosis, and improving responses to immunotherapy.

Stromal cells and immune cells are the two major non-tumor components in TME [11, 12] that significantly influence the invasion and drug resistance of MM [6, 13].

Consequently, evaluating these cellular components in the TME may be beneficial for diagnosis and prognosis prediction in melanoma patients. An ESTIMATE algorithm was developed by Yoshihara et al. for effectively quantifying the proportion of stromal cells and immune cells in TME, thereby offering insights into the TME [14]. Prior studies have demonstrated that TME-related biomarkers screened based on the ESTIMATE algorithm, are effective in diagnosing and predicting the prognosis of various cancers, including glioblastoma [15], breast cancer [16], renal clear cell carcinoma [17], and colon cancer [18]. However, to date, there has been no exploration of its application in MM.

For this study, we sourced RNA-seq data of MM from online databases and utilized the ESTIMATE algorithm to determine immune, stromal, and overall ESTIMATE scores within the TME. Using these scores, alongside various bioinformatics analysis methods, we identified the prognostic marker PTPN6 based on the TME. We then conducted in vitro and in vivo experiments to confirm and investigate its potential molecular biological mechanisms. Our research revealed that the TME-associated gene PTPN6 can inhibit the onset, invasion, and metastasis of MM, thereby improving patient prognosis and response to treatment. Additionally, it was shown that PTPN6 can inhibit the activation of the JAK2-STAT3 signaling pathway. These findings indicate that PTPN6 could act as a new prognostic biomarker for MM. Targeting the PTPN6-JAK2-STAT3 axis in conjunction with immunotherapy could represent an innovative treatment approach to overcome resistance to immunotherapy.

Materials and methods

Data collection

The transcriptome RNA sequencing data and corresponding clinical data of 368 MM samples and 1405 normal skin tissue samples were downloaded from The Cancer Genome Atlas Program (TCGA) (https://portal.gdc.cancer.gov/) and Genotype Tissue Expression (GTEx) (https://www.gtexportal.org/home/index.html) Database. Furthermore, the immunotherapy information of patients with MM was obtained from the Cancer Imaging Archive (TCIA) (https://www.cancerimagingarchive.net/) database.

The identification of differentially expressed genes

The ESTIMATE algorithm was used to assess the TME composition of each MM sample. The results were expressed as three scores, namely ImmuneScore, StromalScore, and ESTIMATEScore. The ImmuneScore and StromalScore correspond to the infiltration level of immune and stromal cells in the TME, respectively. The ESTIMATEScore represents the sum of the immune and stromal scores in individual cases and is defined as tumor purity. According to the analysis results of ESTIMATE, all samples were divided into high/low immune score groups and high/low stromal score groups. Then, the "limma" package in R4.2.3 was used to analyze the differentially expressed genes (DEGs) related to TME by using | log fold change (FC) | > 1.9 and false discovery rate

(FDR) < 0.001 as the cutoff criteria. DEGs with similar levels in stromal and immune cells were screened using the "VennDiagram" package. Heatmaps of TME-related DEGs were generated using the "heatmap" package.

Construction of protein–protein interaction (PPI) network and univariate Cox regression analysis

All DEGs were imported into the STRING online database (https://version-11-5.string-db.org/), a platform designed for identifying interacting genes. We set the interaction's comprehensive score threshold to greater than 0.900 to build a PPI network. This network was then visualized using cytoscape software. Subsequently, core genes within the PPI network, each connected to 15 or more nodes, were continued with univariate Cox regression analysis. Through this process, using a significance threshold of $p < 0.005$, we identified DEGs significantly correlated with the prognosis of MM.

Expression levels and survival analysis of PTPN6 in MM

MM samples in the TCGA database and normal skin tissue samples in the GTEx database were analyzed using the "limma" package to verify the expression level of the PTPN6 gene. Then, according to PTPN6 expression, we performed overall survival (OS) and progression-free survival (PFS) analyses using the "survival" package.

Correlation analysis of PTPN6 with immune cell infiltration and immunotherapy response in MM

We used the Tumor Immune Estimation Resource 2.0 (TIMER2.0) online database (http://timer.cistrome.org/) to analyze the association between PTPN6 expression level and immune infiltration of MM. Concurrently, we used the immunotherapy information data of patients with MM in the TCIA database to conduct correlation analyses between PTPN6 expression and the therapeutic response to immunotherapy.

Cell culture

Human immortalized epidermal keratinocyte cell line (HaCaT) and human metastatic melanoma cell lines (A2058, M14) were obtained from Procell Life Science & Technology Co., Ltd. (Wuhan, China). All cells were cultured in DMEM high-glucose medium (SIGMA, USA) supplemented with 10% Fetal Bovine Serum (FBS) (Excell, USA) and 1% penicillin/streptomycin (SEVEN, Beijing, China).

Cell transfection

The recombinant human full-length PTPN6 gene expression plasmid (pcDNA3.1(+)-PTPN6) and the empty vector plasmid (pcDNA3.1(+)-NC) were synthesized by GenePharma (Shanghai, China). The cells were digested and inoculated on a 6-well plate the day before transfection to ensure that the confluence of the cells reached 60% overnight. Plasmid transfection was performed using the Lipo8000 (Beyotime, Shanghai, China) transfection reagent. After transfection for 48 h, the cells were collected for further analyses.

The PTPN6 overexpression lentivirus (GV341-PTPN6-3FLAG-SV40-puromycin) was obtained from GeneChem (Shanghai, China). 1×10^5 A2058 and M14 cells were inoculated in 6-well plates and cultured until the cell confluence reached 60–70%. According to the manufacturer's instructions, the PTPN6-overexpressing lentivirus was transfected into two melanoma cell lines using the Lipo8000 transfection reagent. After 24 h, the medium was replaced, and cells were screened with 2 μg/mL puromycin. The overexpression efficiency of PTPN6 was verified by Western blotting after one week of screening.

PTPN6 small interfering RNA (siPTPN6) and control siRNA (siNC) were designed and synthesized by GenePharma (Shanghai, China). The sequences of siRNAs were listed in Table S3. A total of 1×10^5 A2058 cells and M14 cells stably overexpressing PTPN6 were inoculated in 6-well plates and cultured until the cell confluence was 60–70%. The siPTPN6 and siNC were transfected into the cells using Lipo8000 transfection reagent. After 48 h of transfection, the knockdown efficiency of PTPN6 was confirmed by Western blotting.

RNA extraction and real-time quantitative polymerase chain reaction (RT-qPCR)

Total RNA was isolated from cells using RNAeasy™ Animal RNA Isolation Kit with Spin Column (Beyotime, Shanghai, China). The concentration of total RNA was measured by NanoDrop ultraviolet spectrophotometer. We reverse transcribed the total RNA into cDNA using the All-in-one first strand cDNA Synthesis Kit II (SEVEN, Beijing, China). The 2 × SYBR Green qPCR Master Mix II kit (SEVEN, Beijing, China) was used for RT-qPCR analysis. Using GAPDH as a reference gene. The $2^{-\Delta\Delta Ct}$ method was used to calculate the relative expression of mRNA. The primers used in the study were as follows: GAPDH, 5'-CTGGGCTACACTGAGCACC-3' (forward) and 5'-AAGTGGTCGTTGAGGGCAATG-3' (reverse); PTPN6, 5'-CTTTGACCACAGCCGAGTGA-3' (forward) and 5'-GCCTAGCAGCTGGTTCTTGA-3' (reverse).

Western blotting

Proteins were extracted from cells using RIPA lysis buffer (Beyotime, Shanghai, China). After that, the obtained proteins were separated using SDS-PAGE and transferred onto a PVDF membrane. The membrane was exposed to the super-sensitive ECL chemiluminescent substrate (Biosharp, Beijing, China) to detect and image protein bands. Finally, we calculated relative protein expression

through gray analysis using ImageJ software. Details of the antibodies used in the study were listed in Table S2.

Cell counting kit 8 (CCK8) assay

The cell growth capability after cell transfection was assessed by the Cell Counting Kit-8 assay kit (Biosharp, Beijing, China). The cells were trypsinized and inoculated in 96-well flat-bottomed plates. Each sample was tested in five replicate wells. At 0, 24, 48, and 72 h after cell adhesion, a fresh complete medium containing 10% CCK8 reagent replaced the old medium and further incubated for an additional 2 h. Then, we measured the optical density (OD) value at a wavelength of 450 nm by an automatic microplate reader.

5-Ethynyl-2′-deoxyuridine (EdU) assay

Cell growth was also determined by EdU incorporation assay, using the BeyoClick™ EdU Cell Proliferation Kit with Alexa Fluor 594 (Beyotime, Shanghai, China). In 24-well plates, cells with different treatments were inoculated at the density of 4×10^4 cells/well. After 24 h, the cells were treated with 10 μM EdU solution and further seeded for another 2 h. The cells were then fixed and were permeabilized with immunostaining permeabilization solution for 15 min. Subsequently, click reaction solution was added, and the cells were incubated in the dark for 30 min. The nucleus was stained with Hoechst 33,342. Finally, the EdU-positive cells were captured under a fluorescence microscope, and five visual fields were randomly selected from each experimental group. The ImageJ software was used to count cells.

Wound healing assay

The ability of cell migration was assessed by a wound healing assay. The cells grew to a confluence of about 90–95% in six-well plates. Then, scratched a wound using a 200 μL pipette tip. Subsequently, after discarding the culture medium, the serum-free DMEM medium was added to each well to continue incubation. The images of the scratch area were taken by microscope at 0, 24, and 48 h, respectively. The ImageJ software was used to measure the wound area.

Transwell migration and invasion assay

For the migration assay, 3×10^4 cells in 200 μL serum-free DMEM medium were added into the upper chamber. The lower chamber was filled with 600 μL complete medium. The medium was discarded after culturing for 24 h, and 4% paraformaldehyde fixed the cells for 30 min. Cells were stained for 20 min with 0.1% violet solution. After being washed twice with PBS, the upper chamber containing non-migrated cells was wiped gently with a cotton swab and dried at room temperature. Subsequently, observations were performed, and photographs were taken using an inverted microscope. Each sample was randomly selected for cell counting in five microscopic fields (× 200). The experiments were conducted in triplicate. For the invasion assay, the upper membrane of the chamber was pre-coated with Matrix-Gel™ Basement Membrane Matrix (Beyotime, Shanghai, China). The remaining steps followed the same protocol as used in the migration assay.

Animals and models

Male BALB/c nude mice (five weeks old) were purchased from Qiguan Biotech (Harbin, China), and were housed in a Specific Pathogen Free animal facility at Harbin Medical University. The facility was maintained on a 12-hour light/dark cycle with a temperature of 22±2 °C and humidity of 50–60%. All animal experiments were conducted in accordance with the principles outlined in the *Guide for the Care and Use of Laboratory Animals* by the National Research Council of the United States. The protocol was approved by the Medical Ethics Committee of the Second Affiliated Hospital of Harbin Medical University (Ethical Review Approval Number: SYDW2024-074).

The nude mice were randomly divided into two experimental groups (5 mice per group). Group 1: Mice were injected subcutaneously with A2058 or M14 melanoma cells (control group), Group 2: Mice were injected subcutaneously with A2058 or M14 cells stably overexpressing PTPN6 (PTPN6 overexpression group). 4×10^6 cells were suspended in 100 μL of sterile PBS and injected subcutaneously into the left axillary region of each mouse to establish a subcutaneous graft tumor model. Tumor diameters were measured with a ruler every 3 days. After 4 weeks, mice were executed, and tumors were excised, weighed, and photographed. Tumor samples were then stored for further histological analysis as needed.

Immunohistochemical (IHC) staining

Tumor tissue samples from each group of nude mice were fixed in 10% formalin for 24 h and then embedded in paraffin to prepare paraffin sections. The sections were dewaxed and rehydrated for immunohistochemical staining. After antigen repair with citrate buffer and blocking with BSA, the sections were incubated with primary antibody at 4 °C overnight. Subsequently, the sections were treated with secondary antibody for 1 h at room temperature. The color was developed using DAB, and counterstaining was performed with hematoxylin. Images were acquired using an inverted microscope and analyzed semi-quantitatively using ImageJ software. Details of the antibodies used in the study were listed in Table S2.

Statistical analysis

R language (version 4.3.1) or GraphPad Prism10.1.1 software was used for statistical analysis. Comparison

between the two groups was analyzed by the student's *t*-test. One-way ANOVA was used for comparison between three groups or more. The data were presented as the mean ± standard deviation (SD). The value of $p<0.05$ was considered statistically significant. We conducted all experiments in triplicate.

Results

ImmuneScore and StromalScore were associated with the prognosis of patients with MM

Based on the TCGA database, we analysed the gene expression and clinical data of 368 patients with SKCM-metastasis by the ESTIMATE algorithm. And we obtained the ImmuneScore, StromalScore, and ESTIMATEScore (Table S1). To study the potential relationship between prognosis and ImmuneScore or StromalScore, according to the median score we divided patients into high and low-score groups for survival analysis. As displayed in Fig. 1A–C, The Kaplan-Meier survival curve indicated the proportion of immune components and the overall survival rate in patients with MM are positively correlated ($p<0.001$). Although the StromalScore did not show a notable correlation with the overall survival rate ($p=0.118$), the ESTIMATEScore, representing the combined total of immune and stromal scores, displayed a positive association with survival ($p<0.001$). These findings suggest that the TME is linked to the prognosis of MM, with the immune elements within the TME being more indicative of prognostic outcomes.

Identification of immune- and stromal-related DEmRNAs for MM

To identify DEGs associated with the TME of MM, according to the high and low immune or stromal scores we performed a differential expression analysis. In this analysis, the immune score group showed 1096 upregulated and three down-regulated genes, while the stromal score group had 777 upregulated and four down-regulated genes. The top 100 differentially expressed genes were displayed in a heatmap (Fig. 1D, E). Using a Venn diagram, we examined the genes common to both immune and stromal groups, identifying 648 upregulated and 0 down-regulated genes (Fig. 1F). These overlapping genes, believed to be crucial DEGs within the microenvironment, were deemed significant in influencing TME. Therefore, our subsequent analyses concentrated on these intersecting genes.

To determine key genes correlated with pathogenesis and survival in metastatic melanoma, we previously utilized the online STRING tool to construct a PPI network of DEGs. This network comprised 112 nodes and 256 edges and was visualized using Cytoscape software (Fig. 1G). As depicted in Fig. 1H, we listed the top 15 genes by nodes in the PPI network, focusing on seven genes with more than 15 nodes for deeper analysis. Concurrently, to identify TME-related genes with prognostic significance, we performed univariate Cox regression analysis on these seven genes. This analysis revealed that LCK, CD247, CD8A, PTPN6, and CD3D were significantly associated with patient prognosis (Fig. 1I). Among these five genes, LCK [19], CD247 [20], CD8A [21], and CD3D [20] have been reported to predict the prognosis of melanoma. However, it remains unclear whether PTPN6 affects the prognosis of MM. Therefore, we decided to focus our subsequent research on PTPN6.

The low expression of PTPN6 in MM was correlated with poor prognosis

We analyzed the RNA sequencing data from TCGA and GTEx databases. The results showed that normal skin tissue expressed significantly higher levels of PTPN6 than MM ($p<0.001$, Fig. 2A). Furthermore, according to the median expression of PTPN6, the samples of MM were divided into high and low-expression groups to evaluate the prognostic value of PTPN6. Subsequently, a survival analysis was conducted. According to the survival curves, there was an increased overall survival ($p<0.001$, Fig. 2B) as well as a greater progression-free survival ($p=0.008$, Fig. 2C) in the high-expression group. The results suggested that a poor prognosis in patients with MM was correlated with a low-expression of PTPN6.

To further confirm the above findings of bioinformatics analyses, we used RT-qPCR and Western blotting assays to detect the expression levels of PTPN6 in the human normal skin keratinocyte line (HaCaT) and two human metastatic melanoma cell lines (A2058 and M14). Compared to the HaCaT cell, the transcription and translation levels of PTPN6 in A2058 and M14 cells were lower (Fig. 2D, E). These results were consistent with our bioinformatics analyses.

To further analyze the role of PTPN6 in MM, we transiently transfected PTPN6 overexpression plasmid and negative control empty vector plasmid into A2058 and M14 cells by Lipo8000 transfection reagent, respectively. RT-qPCR and Western blotting assays were used to detect transfection efficiency. Compared with the control and empty vector plasmid group, the expression level of PTPN6 was notably increased in the pcDNA3.1(+)-PTPN6 transfected group (Fig. 3A-C). The successfully transfected cells were then used in the following experiments.

Overexpression of PTPN6 inhibited the proliferation of MM cells

To validate the effect of PTPN6 overexpression on MM cells proliferation, we conducted the CCK8 assay. The cells transfected with pcDNA3.1(+)-PTPN6 plasmid and empty vector plasmid 12 h were trypsinized and

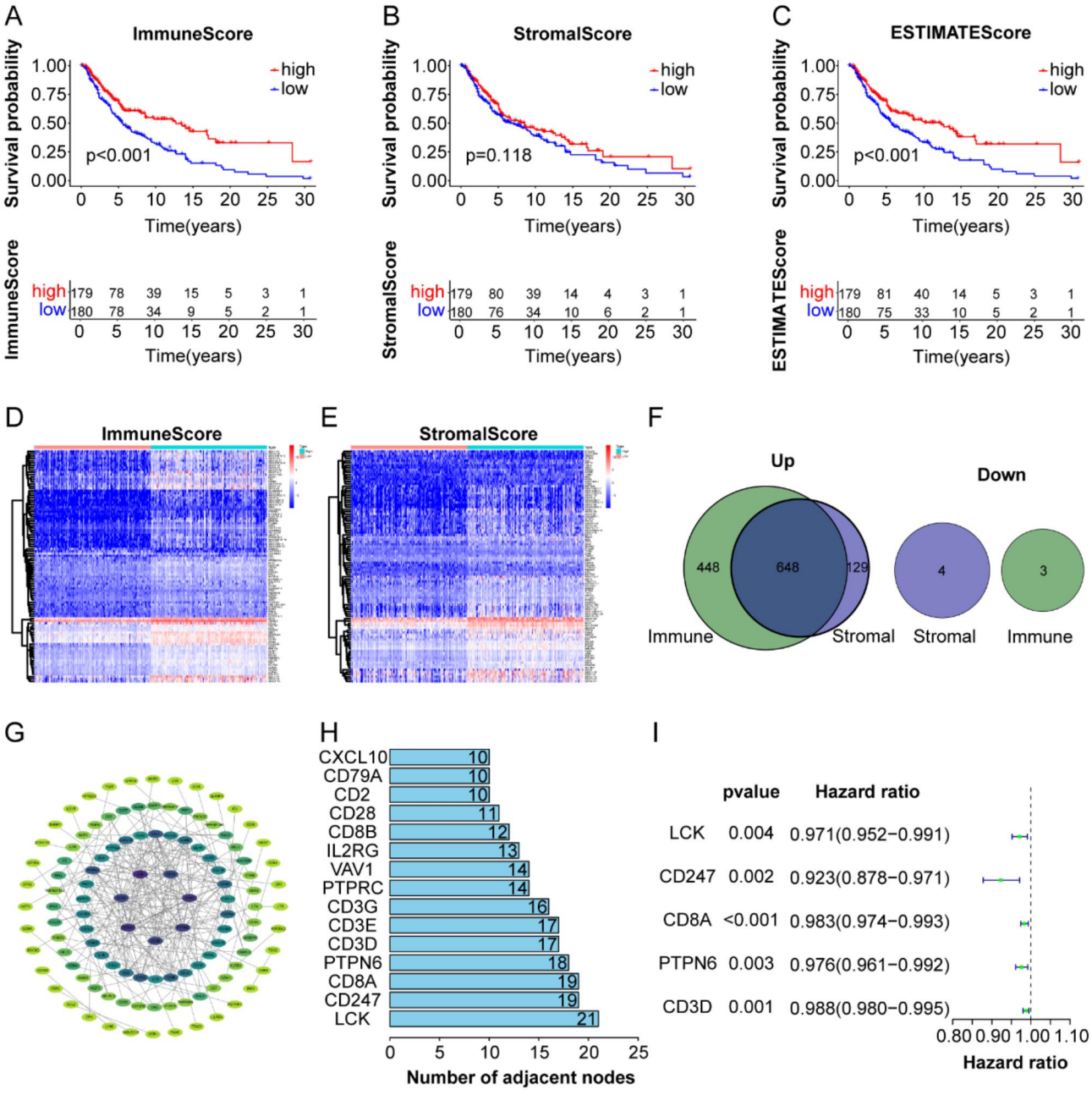

Fig. 1 Identification of differentially expressed genes based on ImmuneScore and StromalScore. (**A-C**) Overall survival analysis of high and low Immune/Stromal/ESTIMATE Scores in patients with metastatic melanoma using the ESTIMATE algorithm. (**D**, **E**) Heatmap depicting the top 100 DEmRNAs with the most significant p-values between high and low Immune/Stromal Scores (|log Fold change|>1.9, $p < 0.001$). Blue represents downregulation, while red represents upregulation. (**F**) Venn diagram showing the upregulated and downregulated genes commonly intersecting between Stromal and Immune Scores, with green indicating immune-related DEmRNAs and purple indicating stromal-related DEmRNAs. (**G**) Construction of a protein-protein interaction network for overlapping genes using the STRING online tool (confidence score > 0.900) and Cytoscape software. (**H**) The top 15 genes ranked by nodes in the PPI network are shown in the graph. (**I**) Univariate Cox analysis was conducted on genes with a node count of 15 or more in the PPI network to identify differentially expressed genes significantly associated with prognosis

reinoculated on a 96-well plate. The growth of the cell was then detected using the CCK8 kit at 0, 24, 48, and 72 h after cell adhesion. According to the results of the experiments, the OD450 values of the cells overexpressed with PTPN6 at the above specific time points were much smaller than those of the control group (Fig. 3D, E). In addition, an EdU incorporation experiment was performed, and the results showed that the percentage of EdU-positive cells in the PTPN6 overexpression group was lower than that in the control group (Fig. 3F, G).

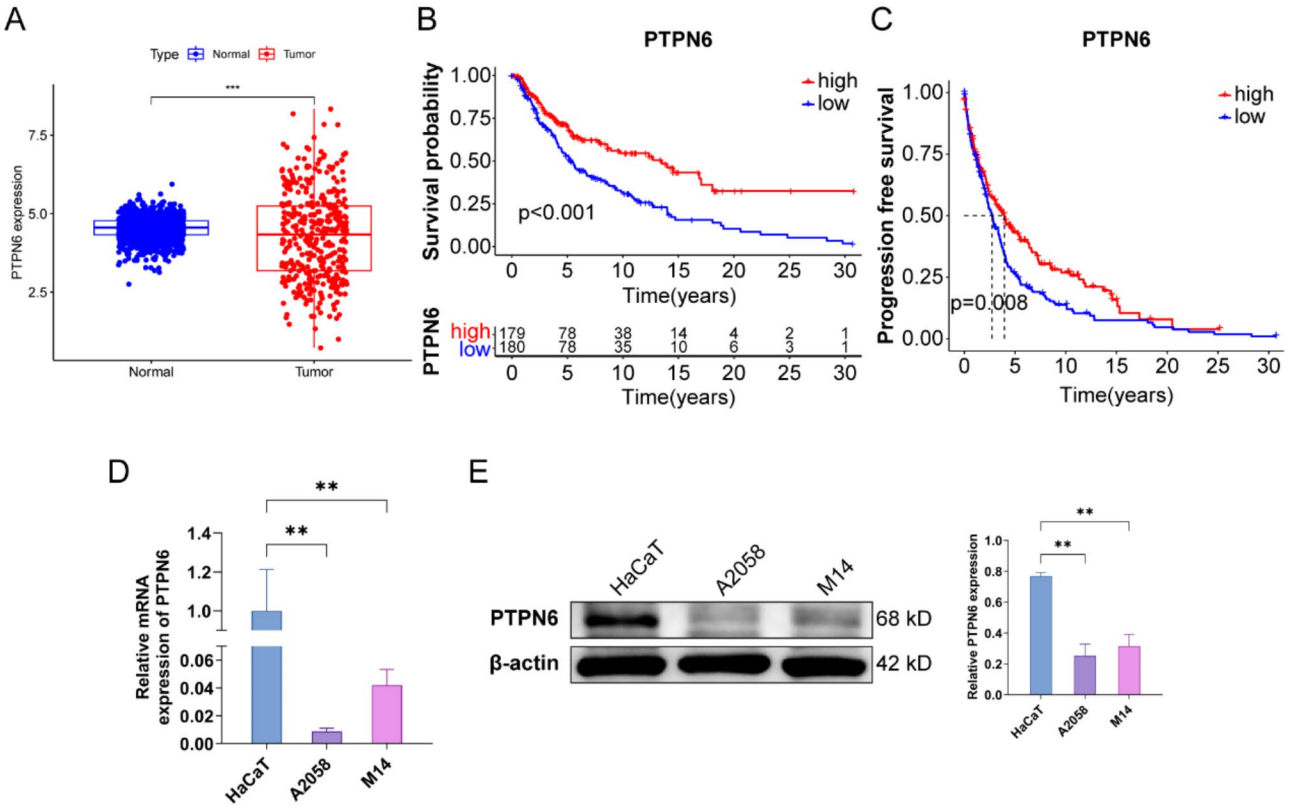

Fig. 2 The expression of PTPN6 and its correlation analysis with survival. (**A**) Boxplot showing differential expression of PTPN6 in metastatic melanoma samples and normal skin tissue samples. (**B**) Correlation analysis of PTPN6 expression in metastatic melanoma samples with overall survival. (**C**) Correlation analysis of PTPN6 expression in metastatic melanoma samples with progression-free survival. (**D**) RT-qPCR assay analyzed the transcription level of PTPN6 in human keratinocyte cell line HaCaT and human metastatic melanoma cell lines A2058 and M14. The RT-qPCR results showed the relative mRNA expression of PTPN6 normalized to GAPDH. (**E**) Western blotting assay analyzed the expression of PTPN6 in human keratinocyte cell line HaCaT and human metastatic melanoma cell lines A2058 and M14. (**$p < 0.01$, ***$p < 0.001$)

These findings indicated that overexpression of PTPN6 in MM cells significantly inhibited cell proliferation ability and cell viability.

Overexpression of PTPN6 inhibited the migration and invasion of MM cells

The wound healing assay, the transwell migration assay, and matrix-gel invasion assay were also used to detect the impact of PTPN6 on the migration of MM cells after transfection with pcDNA3.1(+)-PTPN6 plasmid. As demonstrated by the cell wound healing assay, the PTPN6 overexpression group had significantly larger wound area compared with the control group after 24 and 48 h. However, the wound healing rate slowed (Fig. 4A, B). Additionally, the PTPN6 overexpression group showed a significantly decreased number of migration or invasion cells in the transwell migration and invasion experiments (Fig. 4C, D).

Furthermore, we conducted Western blotting experiments to assess the expression levels of genes implicated in the migration and invasion of cancer cells, specifically focusing on Matrix Metallopeptidase-2,9 (MMP-2,9), E-cadherin, and vimentin. MMP2 and MMP9 are enzymes known for their role in breaking down diverse components of the extracellular matrix, thereby facilitating the growth and infiltration of cancer cells. E-cadherin and vimentin serve as markers of epithelial-mesenchymal transformation (EMT), a process regarded as crucial in tumor invasion and progression. Prior studies have linked EMT to the malignant transformation in metastatic melanoma [22]. As presented in Fig. 4E, F, compared with the control group, the protein expression levels of MMP2, MMP9, and vimentin in the cells transfected with overexpressed PTPN6 plasmid were significantly decreased, while E-cadherin expression level was increased. These findings indicated that PTPN6 suppresses the migration and invasion of MM cells.

Exogenous PTPN6 can inhibit the JAK2-STAT3 pathway in MM cells

In earlier studies, a reduction or absence of PTPN6 was observed in hematopoietic malignancies and colorectal epithelioma cell lines. Additionally, it was found that upregulating PTPN6 could lead to anti-angiogenic and

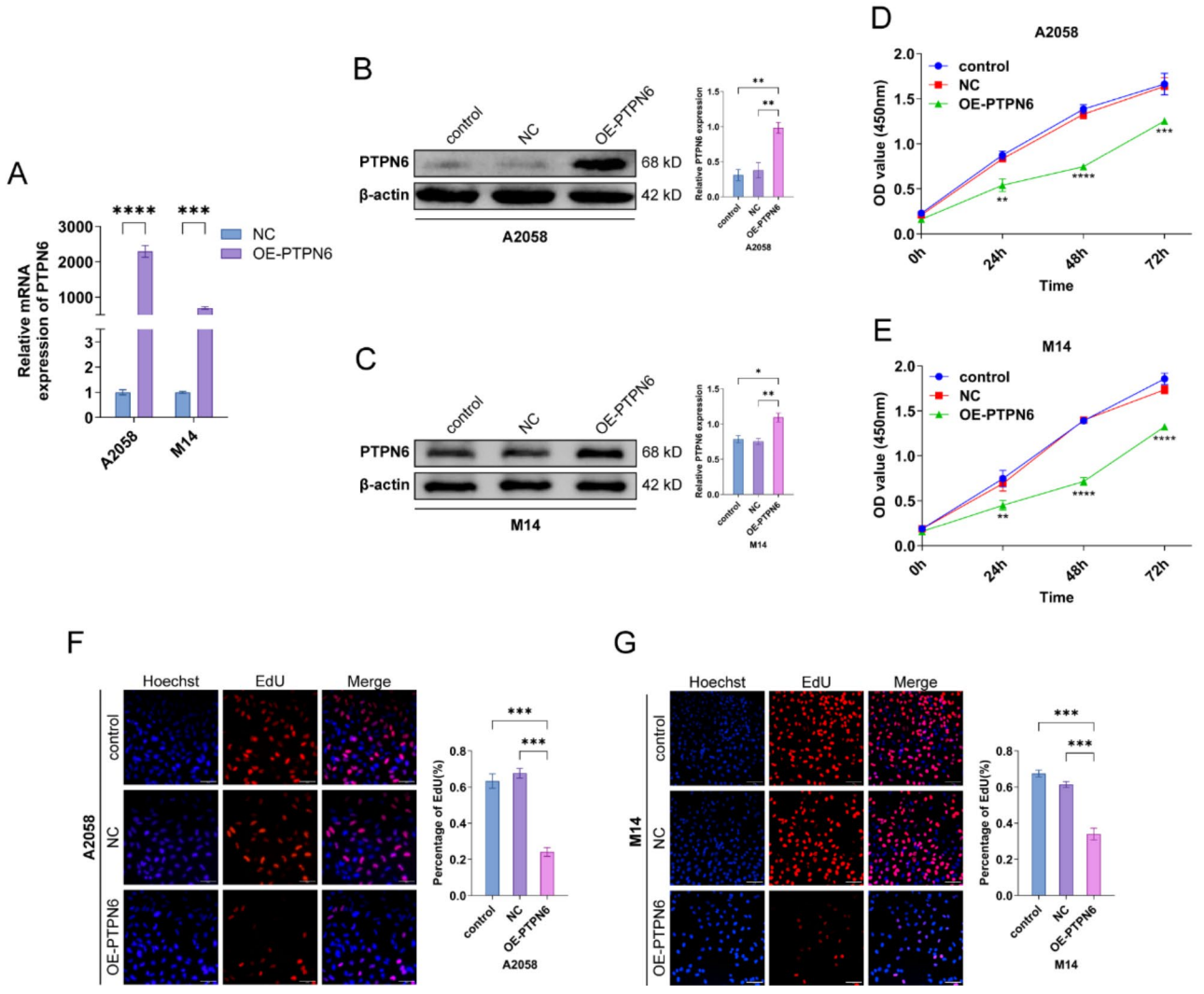

Fig. 3 Overexpression of PTPN6 inhibited the proliferation and viability of metastatic melanoma cells in vitro. (**A–C**) RT-qPCR and Western blotting assays were performed to evaluate the mRNA and protein expression of PTPN6 in A2058 and M14 cells after transfection with PTPN6. The RT-qPCR results showed the relative mRNA expression of PTPN6 normalized to GAPDH. (**D**, **E**) CCK8 assay was used to determine the impact of PTPN6 overexpression on the proliferation of A2058 and M14 cells. (**F**, **G**) EdU assay was conducted to assess the impact of PTPN6 overexpression on the viability of A2058 and M14 cells. Representative images were randomly selected from three independent experiments. Data are presented as the mean ± standard deviation (SD). (*$p < 0.05$, **$p < 0.01$, ***$p < 0.001$, ****$p < 0.0001$)

antitumor effects by inhibiting the JAK2-STAT3 signaling pathway [23, 24]. Based on these insights, we aimed to determine if externally introduced PTPN6 could similarly inhibit the onset and progression of MM by blocking the JAK2-STAT3 pathway. We transfected pcDNA3.1(+)-PTPN6 or pcDNA3.1(+)-NC plasmid into A2058 and M14 cell lines. After 48 h of transfection, we used a Western blotting assay to analyze the activity of the pathway. The expression levels of phosphorylated JAK2 and phosphorylated STAT3 were down-regulated in A2058 and M14 cell lines transfected with pcDNA3.1(+)-PTPN6, but there were no significant changes in the expression of total JAK2 and STAT3 (Fig. 5A-D). These findings suggest that exogenous PTPN6 in MM negatively regulated the pathway through dephosphorylation, thereby further inhibiting the invasion and progression of MM.

There is a significant correlation between the expression of PTPN6 and immune cell infiltration levels and immunotherapy response

Melanoma has strong immunogenicity, can interact with various immune cells, and is sensitive to immunotherapy. However, only a few patients respond to immunotherapy and are prone to drug resistance, possibly associated with the immunosuppressive tumor microenvironment. Therefore, we further analyzed the association between PTPN6 expression and immune infiltration. We used the TIMER2.0 database to explore the correlation between

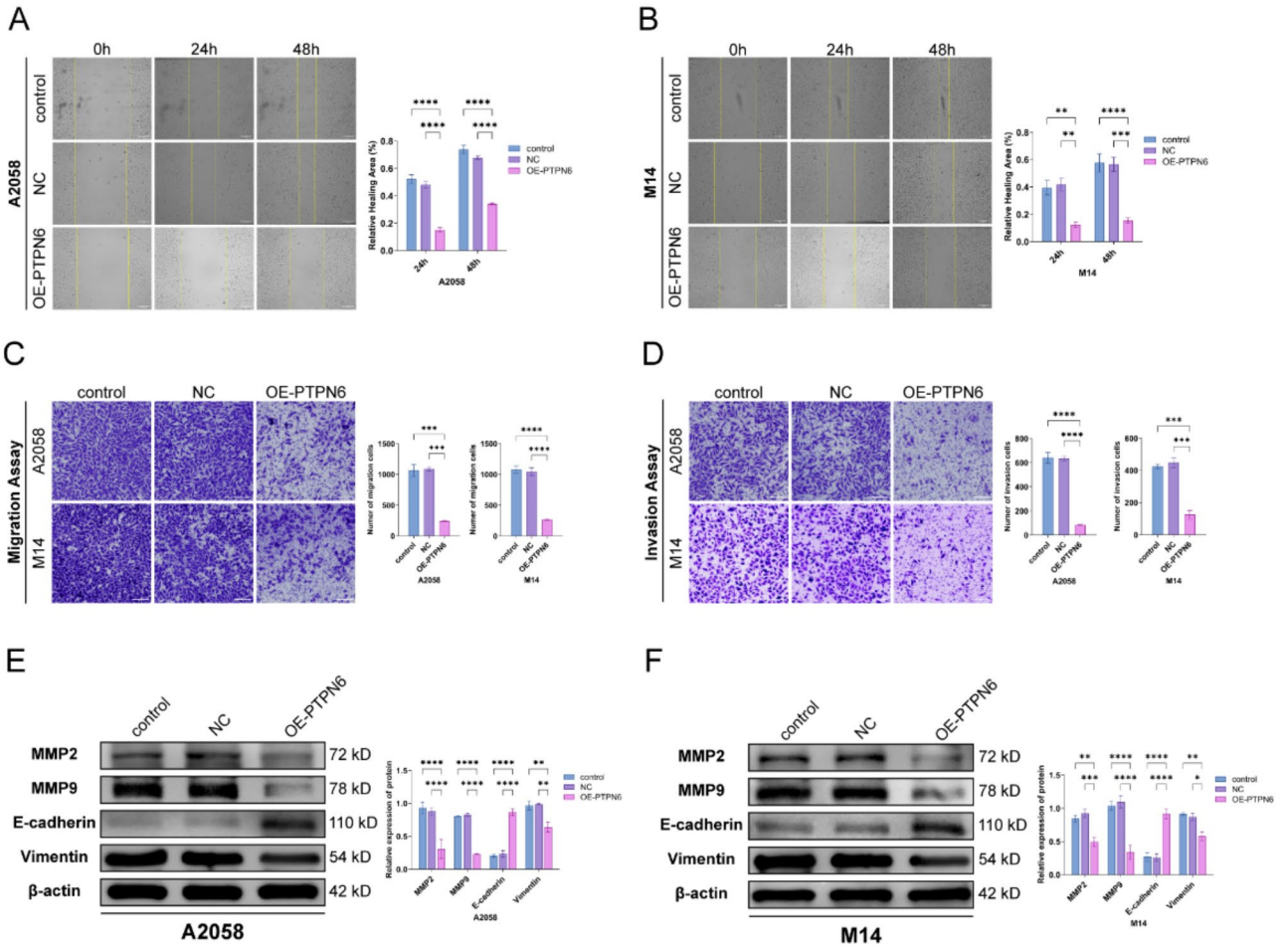

Fig. 4 Overexpression of PTPN6 suppressed the migration and invasion of metastatic melanoma cells in vitro. (**A**, **B**) Wound healing assay was performed to determine the impact of PTPN6 overexpression on the migration of A2058 and M14 cells. (**C**, **D**) Transwell migration and Matrigel invasion assays were used to assess the impact of PTPN6 overexpression on the migration and invasion of A2058 and M14 cells. (**E**, **F**) Western blotting assay was conducted to verify the expression of migration and invasion-related genes, including MMP2, MMP9, E-cadherin, and Vimentin, in control, NC, and PTPN6 overexpression groups in A2058 and M14 cells. Representative images were randomly selected from three independent experiments. Data are presented as mean ± standard deviation (SD). (*$p < 0.05$, **$p < 0.01$, ***$p < 0.001$, ****$p < 0.0001$)

PTPN6 and the abundance of different immune cells. As illustrated in Fig. 6A, PTPN6 expression was negatively associated with tumor purity, myeloid-derived suppressor cells (MDSCs), macrophages M2, and cancer-associated fibroblast. However, PTPN6 positively correlated with activated NK cells, B cells, CD4+T cells, CD8+T cells, macrophages M1, monocyte, myeloid dendritic cells, neutrophils, T cell gamma delta, and T cell follicular helper. These findings further demonstrate that the expression level of PTPN6 impacted the immune status of TME in metastatic melanoma.

Immune checkpoint therapy, as a new immunotherapy method, is crucial in the treatment of MM. Therefore, we downloaded immunotherapy information on patients with MM from the TCIA database and assessed the correlation between PTPN6 expression and immune checkpoint treatment. Our study indicated that patients exhibiting high levels of PTPN6 expression demonstrated improved responses to therapies involving either single-agent CTLA-4, single-agent PD-1, or a combination of both (Fig. 6B). It is suggested that overexpression of PTPN6 could contribute to immunotherapeutic efficacy in patients with MM.

Moreover, we verified the expression of PD-L1, the ligand of immunosuppressive receptor PD-1, by Western blotting assay. It is well established that high expression of PD-L1 can promote immune escape of tumor cells. Our findings indicated that compared to the control group, the cells transfected with pcDNA3.1(+)-PTPN6 plasmid showed decreased levels of PD-L1 expression (Fig. 6C, D).

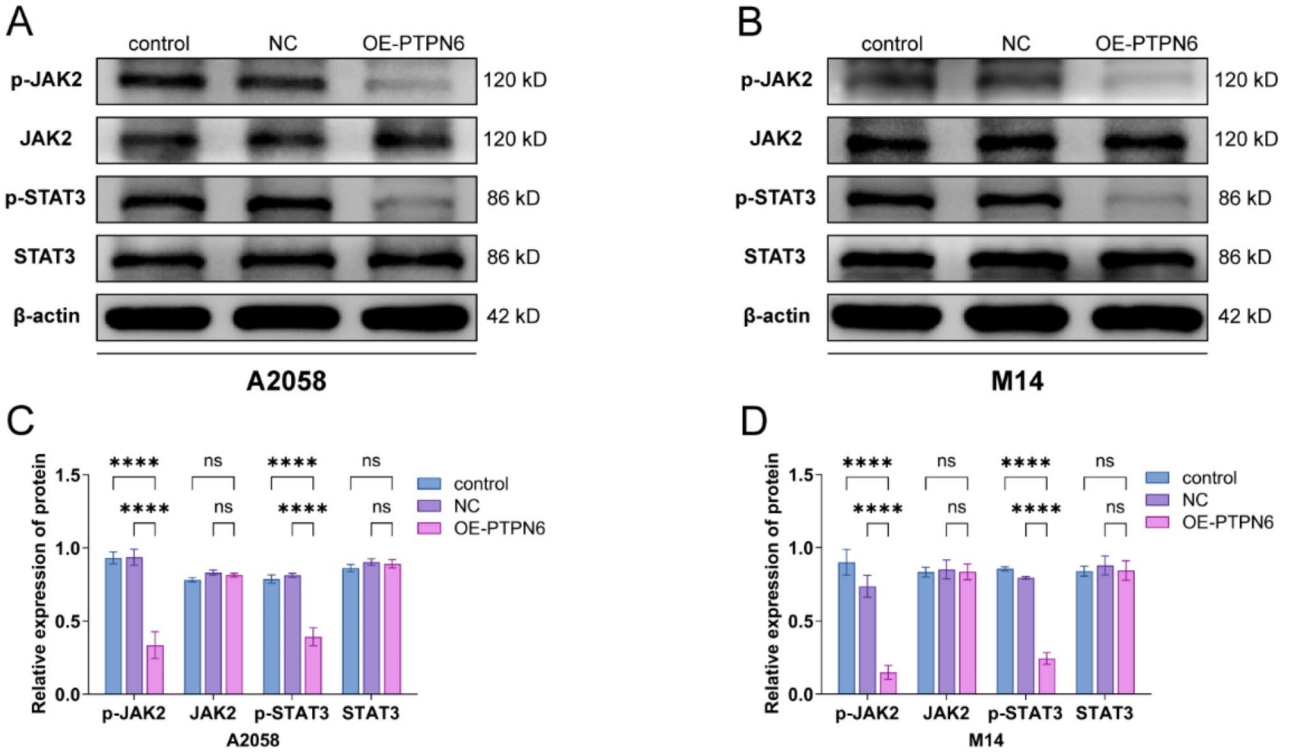

Fig. 5 Overexpression of PTPN6 inhibited the activity of the JAK2-STAT3 signaling pathway in metastatic melanoma cells. (**A-D**) Western blotting assay was used to assess the expression of p-JAK2, JAK2, p-STAT3, and STAT3 after transfection with the PTPN6 overexpression plasmid. (****$p < 0.0001$)

Knockdown of PTPN6 promoted the proliferation, migration, and invasion of MM cells

To further validate the effect of PTPN6 overexpression on the malignant phenotype of MM. We first established A2058 and M14 cell lines stably overexpressing PTPN6 using the GV341-PTPN6-3FLAG-SV40-puromycin lentivirus (Fig. 7A, B). Subsequently, we transiently transfected siPTPN6 into these cell lines (Fig. 7C, D). To observe whether PTPN6 knockdown could reverse its effect on melanoma cell function, we performed CCK8, wound healing, and Transwell assays after the knockdown of PTPN6. The results of CCK8 showed that knockdown of PTPN6 increased the cell proliferation compared to siNC control and PTPN6 overexpression groups (Fig. 7E, F), indicating that reduced PTPN6 expression may promote melanoma cell growth. Wound healing assay showed that at 24 and 48 h after scratching, the wound healing area was smaller in the PTPN6 knockdown group (Fig. 7G, H), suggesting that the knockdown of PTPN6 may promote the migration of MM cells. In the Transwell migration and invasion assay, more cells entered the lower chamber after the knockdown of PTPN6 compared to the PTPN6 overexpression group (Fig. 7I, J), further confirming that the reduction of PTPN6 may enhance the migration and invasion abilities of MM cells.

Overexpression of PTPN6 inhibited MM cells growth in vivo

We subcutaneously injected stable PTPN6 overexpressing melanoma cell lines A2058 and M14, as well as their control cells into the axillae of BALB/c nude mice, respectively, to establish a subcutaneous transplant tumor model. This was done to further investigate whether PTPN6 inhibited melanoma growth in vivo. Tumor diameters were measured with a ruler every three days, and the results were shown in Fig. 8E, F. Tumors in the PTPN6 overexpression group grew more slowly compared to those in the control group. After four weeks, photos were taken to document the overall appearance of the mice and the tumors, and it was evident that the tumors in the control group were larger than those in the PTPN6 overexpression group (Fig. 8A-D). In addition, a similar trend was observed with the tumor weight (Fig. 8G, H). The tumors in the PTPN6-overexpression group weighed less than those in the control group. IHC analysis of paraffin sections of the tumors showed that PTPN6 expression was higher in the overexpression group (Fig. 8I, J). Additionally, Ki67, a marker of cell proliferation, and MMP9, a marker of tumor invasion, were reduced in the PTPN6 overexpression group (Fig. 8I, J). These results suggested that PTPN6 may inhibit the proliferation and invasion of MM cells in vivo.

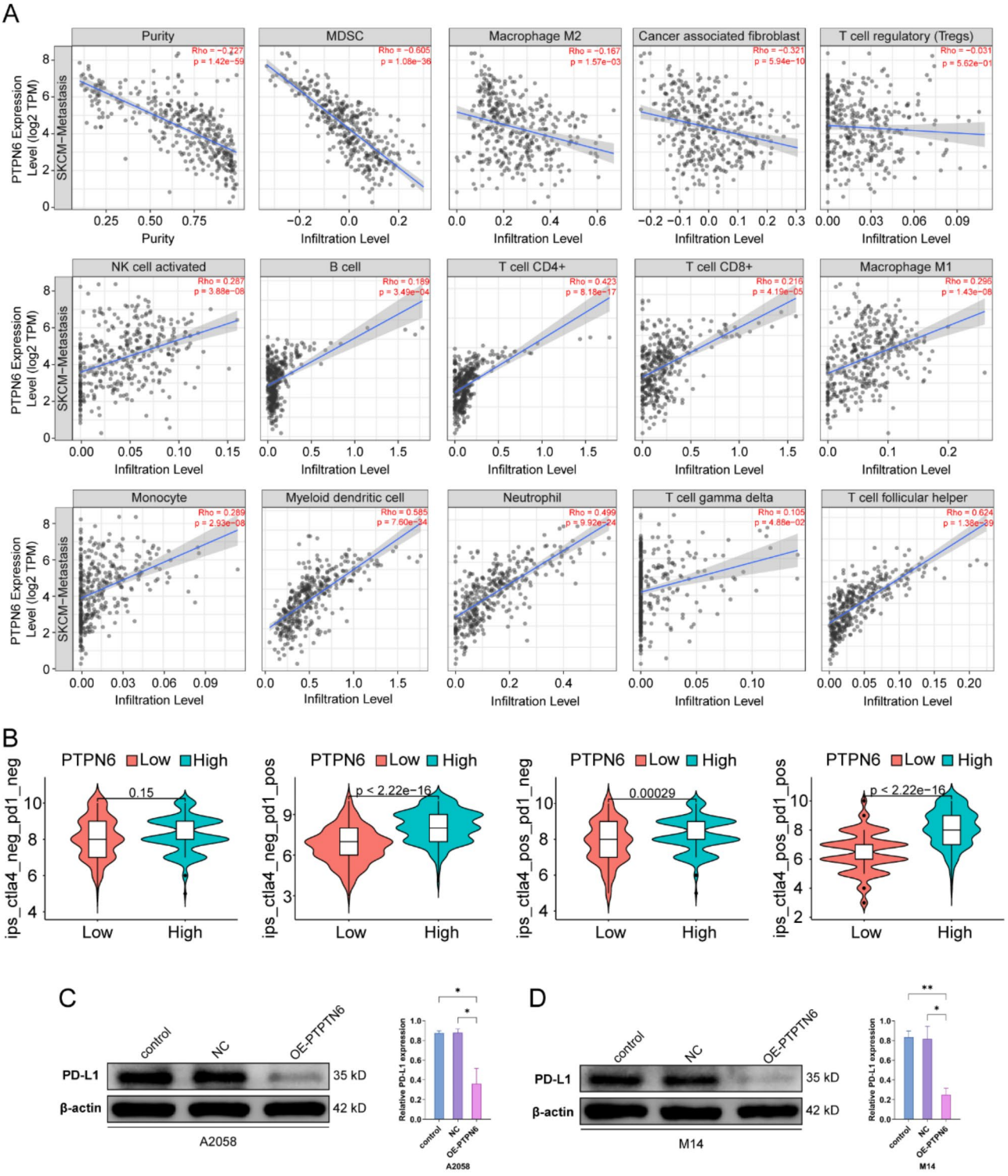

Fig. 6 PTPN6 may affect immune cell infiltration and immune therapy response in metastatic melanoma. (**A**) TIMER 2.0 online analysis tool was used to examine the relationship between PTPN6 and the levels of infiltration of 14 immune cells and tumor purity in metastatic melanoma. (**B**) The correlation between PTPN6 and immune checkpoint therapy (alone or in combination with PD-1 or CTLA-4) response was analyzed using the TCIA database. (**C**, **D**) Western blotting assay was used to detect PD-L1 expression after PTPN6 overexpression (*$p < 0.05$, **$p < 0.01$)

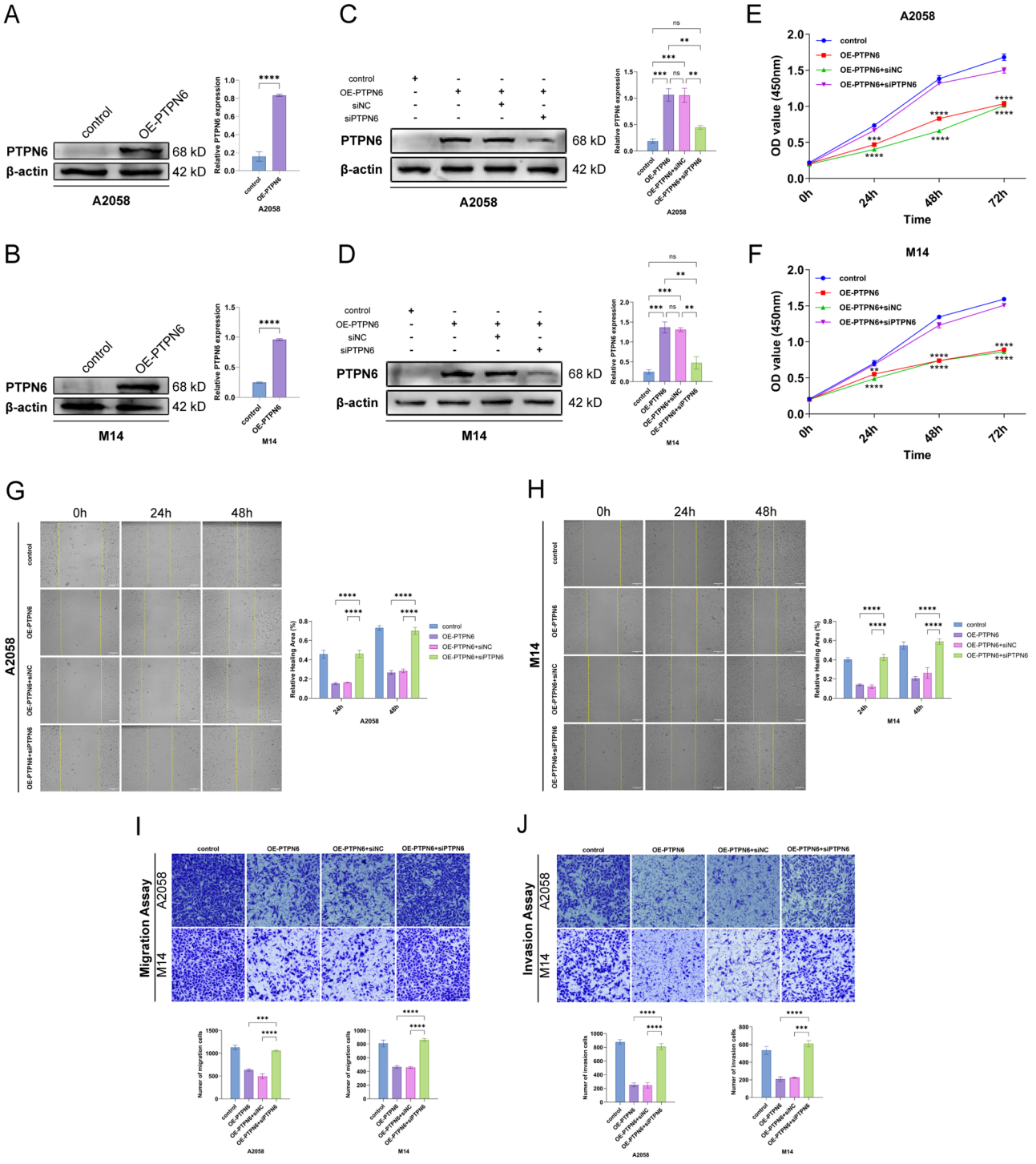

Fig. 7 Knockdown of PTPN6 promoted the proliferation, migration, and invasion of metastatic melanoma cells in vitro. (**A**, **B**) Western blotting assay was performed to evaluate the protein expression of PTPN6 in A2058 and M14 cells after transfection with GV341-PTPN6-3FLAG-SV40-puromycin lentivirus. (**C**, **D**) Western blotting assay was performed to evaluate the protein expression of PTPN6 in A2058 and M14 cell lines stably overexpressing PTPN6 after transiently transfected siPTPN6 or siNC. (**E**, **F**) CCK8 assay was used to determine the impact of PTPN6 knockdown on the proliferation of cells. (**G**, **H**) Wound healing assay was performed to determine the impact of PTPN6 knockdown on the migration of cells. (**I**, **J**) Transwell migration and Matrigel invasion assays were used to assess the impact of PTPN6 knockdown on the migration and invasion of cells. Representative images were randomly selected from three independent experiments. Data are presented as mean ± standard deviation (SD). (**$p < 0.01$, ***$p < 0.001$, ****$p < 0.0001$)

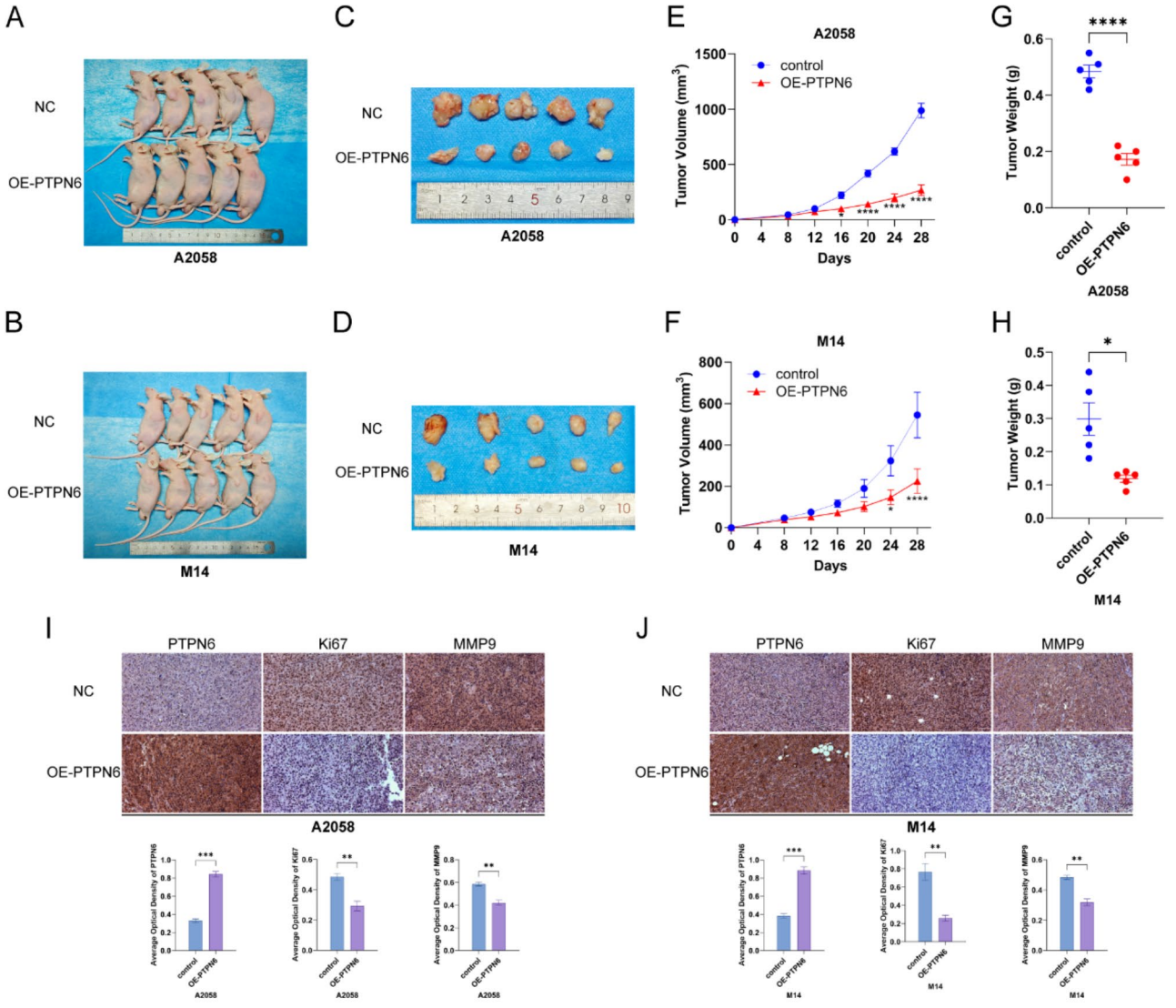

Fig. 8 Overexpression of PTPN6 inhibited the growth of MM cells in vivo. (**A**-**D**) BALB/c nude mice were injected subcutaneously with control and stably PTPN6 overexpressing A2058 or M14 cells. (**E**, **F**) The tumor volume growth curves of mice were plotted. (**G**, **H**) Measurement of mice tumor weight. (**I**, **J**) IHC analysis of PTPN6, Ki67 and MMP9 expressions in tumor tissues. Representative images were randomly selected from three independent experiments. Data are presented as mean ± standard deviation (SD). (*$p < 0.05$, **$p < 0.01$, ***$p < 0.001$, ****$p < 0.0001$)

Discussion

Melanoma is a type of malignant skin tumor with high aggressiveness and is prone to early metastasis, leading to a very high mortality rate. Early localized melanoma, such as stage I and II, generally have a better survival with a five-year survival rate of up to 99.6%. However, for advanced melanoma with lymph node or distant metastasis, the survival is significantly poorer, with a five-year survival rate of only 35.1% for stage IV patients [25].

Conventional treatment approaches for melanoma, including surgical resection, chemotherapy, and radiotherapy, were previously found to have limited effectiveness in managing MM and frequently resulted in severe adverse reactions [4]. Over the past decade, developing numerous targeted therapies and immune-based treatments has substantially enhanced the prospect for treating melanoma [26]. Nevertheless, not all patients were responsive to these treatments, and a considerable number have developed drug resistance and tumor recurrence after a brief period of disease management, factors significantly influenced by the TME of the melanoma [27, 28].

The TME is crucial for the onset and progression of the disease, acting as the nurturing "soil" for tumor cells [8, 12]. Biomarkers associated with the TME may be used to predict survival and response to treatment in patients. However, current studies have ineffectively analyzed the composition of TME in MM. Therefore, our study

comprehensively analyzed the stromal and immune cells, TME-related genes, and clinical survival of patients with MM. This study aimed to identify TME-related genes that could predict MM prognosis using public databases, with validation through in vitro and in vivo experiments.

In this study, first, we analyzed the main cellular components in the TME of MM in the public database by ESTIMATE algorithm and screened out a tumor microenvironment-related prognostic biomarker (PTPN6) by combined PPI network analysis and univariate Cox regression analysis. Then, by analyzing the transcriptome and clinical information of patients with MM in TCGA and GTEx databases, we discovered PTPN6 was low expressed in MM and was linked to negative prognosis. These suggested that PTPN6 may have a tumor-suppressive effect in the occurrence and progression of MM. We then performed in vitro experiments, we first overexpressed PTPN6 in two metastatic melanoma cell lines, and the results revealed that PTPN6 overexpression decreased the growth, migration, and invasion of A2058 and M14 cells. Then, to observe whether PTPN6 knockdown could reverse the effects of PTPN6 overexpression on melanoma cell function, we constructed two melanoma cell lines stably overexpressing PTPN6 and transfected siPTPN6 into each stable cell line to knock down PTPN6. The results showed that the knockdown of PTPN6 enhanced the proliferation, migration, and invasion abilities of MM cells. The inhibitory effect of PTPN6 on the malignant phenotype of A2058 and M14 cells was further corroborated. Next, we constructed a subcutaneous transplant tumor model in nude mice to investigate the effect of PTPN6 on MM in vivo. The results showed that the group injected with MM cells stably overexpressing PTPN6 had slower tumor growth, smaller tumor size, and lower tumor weight compared to the control group. IHC analysis showed that the cell proliferation marker Ki67 and the tumor invasion marker MMP9 were reduced. These findings suggested that PTPN6 may inhibit the proliferation and invasion of MM cells in vivo.

Protein tyrosine phosphatase non-receptor type 6 (PTPN6) belongs to the protein tyrosine phosphatases (PTPs) family. PTPN6 is mainly found in hematopoietic and epithelial cells [29, 30]. It serves as an important regulator of many basic cellular processes, such as growth, development, immune response, and metabolic activities [31], and is widely accepted as a negative regulator of inflammation [32]. PTPN6 shows low expression in most tumors, which may be mainly linked to the abnormal CpG island methylation of its promoter [33, 34]. PTPN6 can antagonize the carcinogenic effect of tyrosine kinase and has been considered as a potential tumor suppressor gene for prostate cancer, colorectal cancer, and other cancers [35]. Furthermore, interestingly, we found that PTPN6 plays a crucial role in immune suppression within the lung cancer microenvironment, primarily through its involvement in CD8+T-cell exhaustion [36]. However, the functional significance and prognostic value of PTPN6 in the malignant transformation of MM remain largely unknown. In this study, we discovered that PTPN6 expression declined in MM patients, and PTPN6 not only predicted the overall survival but also acted as a tumor suppressor for MM occurrence and development. This study highlighted that PTPN6 can be served as a promising prognostic biomarker and therapeutic target for MM.

The JAK/STAT3 pathway is often over-activated in most cancers, including melanoma. It drives carcinogenesis and progression by inhibiting apoptosis and promoting proliferation, angiogenesis, and invasion [37, 38]. Apart from the direct carcinogenic characteristics described above, the JAK/STAT3 pathway is correlated with the immunosuppression of tumors [39]. In the tumor microenvironment, abnormal STAT3 expression was often found in various immune cells. For example, STAT3 activation in dendritic cells reduces the expression of MHCII, CD80, and IL-12, inhibiting their ability to activate T cells and produce an antitumor immune response [40]. STAT3 can also bind to the first intron of the FoxP3 gene and produce immunosuppressive factors such as TGF-β and IL-10 to activate Tregs and promote tumors [41]. Furthermore, studies have shown that the Th17 immune subset activated through this pathway can enhance the progression of melanoma [42]. Therefore, the JAK/STAT3 signal pathway is closely related to the onset and progression of MM.

Previous studies have found that PTPN6 can bind to members of the JAK family and regulate the activity of JAK. The reduction or loss of PTPN6 will increase JAK activity and directly lead to abnormal cell growth [43]. Furthermore, the primary phosphorylation sites for STAT3 are Tyr705 and Ser727, and PTPN6 can dephosphorylate STAT3 at Tyr705 [30], thereby inhibiting the downstream pathway. Recent studies have shown that the reduction or loss of PTPN6 in hematopoietic malignancies or colorectal cancer cell lines and upregulation of PTPN6 can exert anti-angiogenic and antitumor effects by inhibiting JAK2-STAT3 signal transduction [23, 24]. These studies strongly suggest that PTPN6 is a negative regulatory factor of the JAK/STAT pathway. To study whether PTPN6 also exerts a tumor-suppressive effect in MM by inhibiting this signaling pathway, we transfected metastatic melanoma cells with PTPN6 overexpression plasmid. We monitored the expression of genes related to this pathway by Western blotting assays. Our findings indicate that the overexpression of PTPN6 suppressed the levels of p-JAK2 and p-STAT3. However, the overall expression of JAK2 and STAT3 remained relatively unchanged. This suggests that PTPN6 has a crucial role

in suppressing the activation of the JAK/STAT3 pathway in MM. Therefore, PTPN6 can be served as a new prognostic biomarker for human metastatic melanoma, and targeting the PTPN6-JAK2-STAT3 axis may offer a hopeful strategy to enhance the therapeutic effect. A recent study has shown that multikinase inhibitor Sorafenib and its derivative SC-43 enhance the phosphatase function of PTPN6 in hepatocellular carcinoma, thereby inhibiting the activity of p-STAT3 and inducing apoptosis and other anti-hepatoma effects [44]. Moreover, studies have found that Guggulsterone [45] (a phytosteroid extracted from plants) and Plumbagin [46] (a vitamin K3 analog extracted from medicinal plants) exert antitumor effects by inducing the expression of PTPN6.

Recently, immunotherapy has played an increasingly crucial role in melanoma treatment, among which the application of ICIs has become the standard treatment for MM, such as anti-PD-1/PD-L1, anti-CTLA-4, and anti-LAG-3 antibodies have received approval from FDA for treating melanoma [47]. Consequently, we used TIMER2.0 and TCIA databases to assess the relationship between PTPN6 and immune infiltration and immunotherapy. In our study, we measured PD-L1 expression using Western blotting experiments. PD-L1, a ligand for the immunosuppressive receptor PD-1, is often found to be overexpressed in tumor cells. Within the tumor microenvironment, PD-L1 binds to the PD-1 receptor on T cells, resulting in the inhibition of T cell activation and cytokine production. This results in the dysfunction and exhaustion of T cell, inhibiting cytotoxic T cells efficiently attacking tumor cells and thus facilitating the immune evasion of tumor cells. Our findings revealed that the expression of PTPN6 was inversely associated with MDSCs and other immunosuppressive cells and positively connected to the effectiveness of immune checkpoint therapy. PTPN6 overexpression resulted in reduced PD-L1 levels, suggesting that PTPN6 could play a role in inhibiting immune evasion and improving the effects of immunotherapy in melanoma patients.

However, there are still several limitations in this study. The study primarily used a retrospective cohort for analysis, and it may be necessary to require additional prospective cohorts of patients to further confirm the results. Although we discovered the role of PTPN6 in the prognosis and immunotherapy of metastatic melanoma by the analysis of public databases, as well as in vivo and in vitro experiments, further confirmation in clinical samples is necessary. Therefore, in our upcoming research endeavors, we plan to collect extensive clinical patient tissue samples for experimental analysis. Additionally, we will conduct patient follow-ups to collect clinical data to further validate our findings.

Conclusion

To conclude, our study potentially identified a new prognostic biomarker related to the tumor microenvironment, PTPN6, for MM. We found that its expression is typically low in MM and correlates with an unfavorable prognosis. Upregulating PTPN6 expression was observed to inhibit the proliferation, migration, and invasion of metastatic melanoma cells, and it also impeded the activity of the JAK2-STAT3 signaling pathway. PTPN6 knockdown could reverse the effects of PTPN6 overexpression on MM cells. A significant link was also established between PTPN6 and both immune cell infiltration and the response to immunotherapy. Therefore, PTPN6 could be considered a novel therapeutic target and prognostic marker for MM.

Abbreviations

DEGs	Differentially expressed genes
EMT	Epithelial-mesenchymal transformation
GTEx	Genotype Tissue Expression
ICIs	Immune checkpoint inhibitors
MDSCs	Myeloid-derived suppressor cells
MMP-2,9	Matrix Metallopeptidase-2,9
OS	Overall survival
PFS	Progression-free survival
PPI	Protein-protein interaction
PTPN6	Protein tyrosine phosphatase non-receptor type 6
PTPs	Protein tyrosine phosphatases
TCGA	The Cancer Genome Atlas Program
TCIA	The Cancer Imaging Archive
TIMER2.0	Tumor Immune Estimation Resource 2.0
TME	Tumor microenvironment

Supplementary Information

The online version contains supplementary material available at https://doi.org/10.1186/s12935-024-03625-6.

Supplementary Material 1: Table S1. ImmuneScore, StromalScore, and ESTIMATEScore.

Supplementary Material 2: Table S2. Antibodies used in this study.

Supplementary Material 3: Table S3. siRNAs sequences used in this study.

Acknowledgements

We are grateful to all researchers and staff of the mentioned software and databases.

Author contributions

SRY was responsible for the overall design, experimental validation, and manuscript writing of the study. WSQ and YY handled the bioinformatics data processing. WZ was in charge of animal experiments. YTH, ZYN, and CLP were in charge of the statistical analysis of experimental data. MX supervised and funded the project. All authors reviewed the manuscript.

Funding

This study was supported by the Natural Science Foundation of Heilongjiang Province of China (LH2019H069), the China Postdoctoral Science Foundation (2019M661299), and the Young and Middle-aged Innovative Scientific Research Fund of the Second Affiliated Hospital of Harbin Medical University (KYCX2018-05).

Data availability

All datasets analyzed during the current study are available from the above-mentioned public, open access repositories. The R and other custom scripts

used for data analysis can be obtained from the corresponding authors upon reasonable request.

Declarations

Ethics approval and consent to participate
All animal experiments were approved by the Medical Ethics Committee of the Second Affiliated Hospital of Harbin Medical University (Ethical Review Approval Number: SYDW2024-074).

Consent for publication
All authors gave their consent for publication.

Competing interests
The authors declare no competing interests.

Received: 6 March 2024 / Accepted: 17 December 2024
Published online: 28 December 2024

References

1. Garbe C, Amaral T, Peris K, Hauschild A, Arenberger P, Basset-Seguin N, et al. European consensus-based interdisciplinary guideline for melanoma. Part 1: Diagnostics: Update 2022. Eur J Cancer. 2022;170:236–55.
2. Long GV, Swetter SM, Menzies AM, Gershenwald JE, Scolyer RA. Cutaneous melanoma. Lancet. 2023;402(10400):485–502.
3. Garbe C, Amaral T, Peris K, Hauschild A, Arenberger P, Basset-Seguin N, et al. European consensus-based interdisciplinary guideline for melanoma. Part 2: treatment - update 2022. Eur J Cancer. 2022;170:256–84.
4. Davis LE, Shalin SC, Tackett AJ. Current state of melanoma diagnosis and treatment. Cancer Biol Ther. 2019;20(11):1366–79.
5. Eddy K, Chen S. Overcoming Immune Evasion in Melanoma. Int J Mol Sci. 2020;21(23):8984.
6. Falcone I, Conciatori F, Bazzichetto C, Ferretti G, Cognetti F, Ciuffreda L, et al. Tumor Microenvironment: implications in Melanoma Resistance to targeted therapy and immunotherapy. Cancers (Basel). 2020;12(10):2870.
7. Kalaora S, Nagler A, Wargo JA, Samuels Y. Mechanisms of immune activation and regulation: lessons from melanoma. Nat Rev Cancer. 2022;22(4):195–207.
8. Pitt JM, Marabelle A, Eggermont A, Soria JC, Kroemer G, Zitvogel L. Targeting the tumor microenvironment: removing obstruction to anticancer immune responses and immunotherapy. Ann Oncol. 2016;27(8):1482–92.
9. de Visser KE, Joyce JA. The evolving tumor microenvironment: from cancer initiation to metastatic outgrowth. Cancer Cell. 2023;41(3):374–403.
10. Belli C, Trapani D, Viale G, D'Amico P, Duso BA, Della Vigna P, et al. Targeting the microenvironment in solid tumors. Cancer Treat Rev. 2018;65:22–32.
11. Wu T, Dai Y. Tumor microenvironment and therapeutic response. Cancer Lett. 2017;387:61–8.
12. Yuan Y, Jiang YC, Sun CK, Chen QM. Role of the tumor microenvironment in tumor progression and the clinical applications (review). Oncol Rep. 2016;35(5):2499–515.
13. Pulluri B, Kumar A, Shaheen M, Jeter J, Sundararajan S. Tumor microenvironment changes leading to resistance of immune checkpoint inhibitors in metastatic melanoma and strategies to overcome resistance. Pharmacol Res. 2017;123:95–102.
14. Yoshihara K, Shahmoradgoli M, Martínez E, Vegesna R, Kim H, Torres-Garcia W, et al. Inferring tumour purity and stromal and immune cell admixture from expression data. Nat Commun. 2013;4:2612.
15. Jia D, Li S, Li D, Xue H, Yang D, Liu Y. Mining TCGA database for genes of prognostic value in glioblastoma microenvironment. Aging. 2018;10(4):592–605.
16. Li B, Geng R, Wu Q, Yang Q, Sun S, Zhu S, et al. Alterations in Immune-related genes as potential marker of prognosis in breast Cancer. Front Oncol. 2020;10:333.
17. Xu WH, Xu Y, Wang J, Wan FN, Wang HK, Cao DL, et al. Prognostic value and immune infiltration of novel signatures in clear cell renal cell carcinoma microenvironment. Aging. 2019;11(17):6999–7020.
18. Alonso MH, Aussó S, Lopez-Doriga A, Cordero D, Guinó E, Solé X, et al. Comprehensive analysis of copy number aberrations in microsatellite stable colon cancer in view of stromal component. Br J Cancer. 2017;117(3):421–31.
19. Wang F, Zheng A, Zhang D, Zou T, Xiao M, Chen J, et al. Molecular profiling of core immune-escape genes highlights LCK as an immune-related prognostic biomarker in melanoma. Front Immunol. 2022;13:1024931.
20. Bogunovic D, O'Neill DW, Belitskaya-Levy I, Vacic V, Yu YL, Adams S, et al. Immune profile and mitotic index of metastatic melanoma lesions enhance clinical staging in predicting patient survival. Proc Natl Acad Sci U S A. 2009;106(48):20429–34.
21. Wang X, Chai Z, Li Y, Long F, Hao Y, Pan G, et al. Identification of potential biomarkers for Anti-PD-1 therapy in melanoma by Weighted Correlation Network Analysis. Genes (Basel). 2020;11(4):435.
22. Pearlman RL, Montes de Oca MK, Pal HC, Afaq F. Potential therapeutic targets of epithelial-mesenchymal transition in melanoma. Cancer Lett. 2017;391:125–40.
23. Han Y, Amin HM, Franko B, Frantz C, Shi X, Lai R. Loss of SHP1 enhances JAK3/STAT3 signaling and decreases proteosome degradation of JAK3 and NPM-ALK in ALK + anaplastic large-cell lymphoma. Blood. 2006;108(8):2796–803.
24. Xiong H, Chen ZF, Liang QC, Du W, Chen HM, Su WY, et al. Inhibition of DNA methyltransferase induces G2 cell cycle arrest and apoptosis in human colorectal cancer cells via inhibition of JAK2/STAT3/STAT5 signalling. J Cell Mol Med. 2009;13(9B):3668–79.
25. Huang J, Chan SC, Ko S, Lok V, Zhang L, Lin X, et al. Global incidence, mortality, risk factors and trends of Melanoma: a systematic analysis of registries. Am J Clin Dermatol. 2023;24(6):965–75.
26. Jenkins RW, Fisher DE. Treatment of Advanced Melanoma in 2020 and Beyond. J Invest Dermatol. 2021;141(1):23–31.
27. Huang L, Xu Y, Fang J, Liu W, Chen J, Liu Z, et al. Targeting STAT3 abrogates Tim-3 Upregulation of Adaptive Resistance to PD-1 Blockade on Regulatory T Cells of Melanoma. Front Immunol. 2021;12:654749.
28. Hossain SM, Eccles MR. Phenotype switching and the Melanoma Microenvironment; impact on Immunotherapy and Drug Resistance. Int J Mol Sci. 2023;24:1601.
29. Honorat JF, Ragab A, Lamant L, Delsol G, Ragab-Thomas J. SHP1 tyrosine phosphatase negatively regulates NPM-ALK tyrosine kinase signaling. Blood. 2006;107(10):4130–8.
30. Fan LC, Shiau CW, Tai WT, Hung MH, Chu PY, Hsieh FS, et al. SHP-1 is a negative regulator of epithelial-mesenchymal transition in hepatocellular carcinoma. Oncogene. 2015;34(41):5252–63.
31. Chong ZZ, Maiese K. The src homology 2 domain tyrosine phosphatases SHP-1 and SHP-2: diversified control of cell growth, inflammation, and injury. Histol Histopathol. 2007;22(11):1251–67.
32. An H, Hou J, Zhou J, Zhao W, Xu H, Zheng Y, et al. Phosphatase SHP-1 promotes TLR- and RIG-I-activated production of type I interferon by inhibiting the kinase IRAK1. Nat Immunol. 2008;9(5):542–50.
33. Liu L, Zhang S, Liu X, Liu J. Aberrant promoter 2 methylation–mediated downregulation of protein tyrosine phosphatase, non–receptor type 6, is associated with progression of esophageal squamous cell carcinoma. Mol Med Rep. 2019;19(4):3273–82.
34. Li Y, Yang L, Pan Y, Yang J, Shang Y, Luo J. Methylation and decreased expression of SHP-1 are related to disease progression in chronic myelogenous leukemia. Oncol Rep. 2014;31(5):2438–46.
35. Bollu LR, Mazumdar A, Savage MI, Brown PH. Molecular pathways: targeting protein tyrosine phosphatases in Cancer. Clin Cancer Res. 2017;23(9):2136–42.
36. Peng DH, Rodriguez BL, Diao L, Chen L, Wang J, Byers LA, et al. Collagen promotes anti-PD-1/PD-L1 resistance in cancer through LAIR1-dependent CD8(+) T cell exhaustion. Nat Commun. 2020;11:4520.
37. Johnson DE, O'Keefe RA, Grandis JR. Targeting the IL-6/JAK/STAT3 signalling axis in cancer. Nat Rev Clin Oncol. 2018;15(4):234–48.
38. Huynh J, Etemadi N, Hollande F, Ernst M, Buchert M. The JAK/STAT3 axis: a comprehensive drug target for solid malignancies. Semin Cancer Biol. 2017;45:13–22.
39. Zou S, Tong Q, Liu B, Huang W, Tian Y, Fu X. Targeting STAT3 in Cancer Immunotherapy. Mol Cancer. 2020;19(1):145.
40. Kortylewski M, Kujawski M, Wang T, Wei S, Zhang S, Pilon-Thomas S, et al. Inhibiting Stat3 signaling in the hematopoietic system elicits multicomponent antitumor immunity. Nat Med. 2005;11(12):1314–21.
41. Wang Y, Shen Y, Wang S, Shen Q, Zhou X. The role of STAT3 in leading the crosstalk between human cancers and the immune system. Cancer Lett. 2018;415:117–28.
42. Kong LY, Abou-Ghazal MK, Wei J, Chakraborty A, Sun W, Qiao W, et al. A novel inhibitor of signal transducers and activators of transcription 3 activation is efficacious against established central nervous system melanoma and inhibits regulatory T cells. Clin Cancer Res. 2008;14(18):5759–68.

43. Huang TT, Su JC, Liu CY, Shiau CW, Chen KF. Alteration of SHP-1/p-STAT3 signaling: a potential target for Anticancer Therapy. Int J Mol Sci. 2017;18(6):1234.
44. Chao TI, Tai WT, Hung MH, Tsai MH, Chen MH, Chang MJ, et al. A combination of sorafenib and SC-43 is a synergistic SHP-1 agonist duo to advance hepatocellular carcinoma therapy. Cancer Lett. 2016;371(2):205–13.
45. Ahn KS, Sethi G, Sung B, Goel A, Ralhan R, Aggarwal BB. Guggulsterone, a farnesoid X receptor antagonist, inhibits constitutive and inducible STAT3 activation through induction of a protein tyrosine phosphatase SHP-1. Cancer Res. 2008;68(11):4406–15.
46. Sandur SK, Pandey MK, Sung B, Aggarwal BB. 5-hydroxy-2-methyl-1,4-naphthoquinone, a vitamin K3 analogue, suppresses STAT3 activation pathway through induction of protein tyrosine phosphatase, SHP-1: potential role in chemosensitization. Mol Cancer Res. 2010;8(1):107–18.
47. Paik J. Nivolumab Plus Relatlimab: first approval. Drugs. 2022;82(8):925–31.

Publisher's note